

Nonequilibrium nonlinear effects and dynamical boson condensation in a driven-dissipative Wannier-Stark lattice

Arkadiusz Kosior, Karol Gietka , Farokh Mivehvar , and Helmut Ritsch 
Institut für Theoretische Physik, Universität Innsbruck, A-6020 Innsbruck, Austria

 (Received 3 May 2024; revised 12 July 2024; accepted 16 August 2024; published 10 September 2024)

Driven-dissipative light-matter systems can exhibit collective nonequilibrium phenomena due to loss and gain processes on the one hand and effective photon-photon interactions on the other hand. As a generic example we study a bosonic lattice system implemented via an array of driven-dissipative coupled nonlinear resonators with linearly increasing resonance frequencies across the lattice. The model also describes a driven-dissipative Bose-Hubbard model in a tilted potential *without* a particle-conservation constraint. We numerically predict a diverse range of stationary and nonstationary states resulting from the interplay of the tilt, tunneling, on-site interactions, and loss and gain processes. Our key finding is that, under weak on-site interactions, the bosons mostly condense into a selected, single-particle Wannier-Stark state without exhibiting the expected Bloch oscillations. As the strength of the on-site interactions increase, a nonstationary regime emerges which, surprisingly, exhibits periodic Bloch-type oscillations. As a direct consequence of the driven-dissipative nature of the system we predict a highly nontrivial phase diagram including regular oscillating as well as chaotic dynamical regimes. While a straightforward photonic implementation using microwave or optical modes is possible, such dynamics might also be observable for an ultracold gas in a vertical lattice with gravity or a tilted external potential.

DOI: [10.1103/PhysRevB.110.L100303](https://doi.org/10.1103/PhysRevB.110.L100303)

Introduction. The Bose-Hubbard model is a paradigmatic model in condensed-matter physics for describing strongly correlated interacting bosons on a lattice [1,2]. Dissipative behavior in these systems, typically induced by coupling with external degrees of freedom, lead to a range of complex phenomena, including emergent phase transitions [3–5], pair coherent states [5], dissipation-induced correlations [6], and pair condensation within density-induced tunneling where dissipation can emerge intrinsically [7,8]. Given that the Bose-Hubbard model is well-suited for bosonic systems, could it (or similar models) also be used to describe strongly correlated multiphoton states? Although photons do not directly interact with each other, they can effectively interact through their interaction with matter (particularly in nonlinear Kerr media), which could give rise to intriguing collective phenomena analogous to condensate matter. Indeed, this research direction was postulated almost 20 years ago [9,10] and has been actively developed since then [11,12].

Nevertheless there is a major difference between particle and photon systems: while the matter-particle number is strictly conserved, photons can appear and disappear due to absorption, spontaneous or stimulated emission, and external photon sources. This causes open photonic systems to be inherently out of equilibrium [13] and even stationary states are typically not determined simply by temperature and entropy, but rather by the dynamical balance of gain and loss. Intriguing nonequilibrium phenomena can thus appear in composite light-matter systems [14–17] and, in particular, in quantum fluids of light [18]. The most notable example is the observation of the quasiequilibrium Bose-Einstein condensate (BEC) of exciton polaritons—bosonic quasiparticles composed of a mixture of an exciton (an electron-hole pair) and a cavity photon—in a semiconductor microcavity [19–22] and

the BEC of photons interacting via molecules in a multimode optical microcavity [23]. Despite the driven-dissipative nature of these systems, they still exhibit an effective thermalization process to which one can attribute an effective temperature. This stands in a sharp contrast to a typical laser operation, where the thermalization is completely ineffective and the photon gas is far out-of-equilibrium.

Finally, substantial progress has been achieved in investigating correlated many-body effects with photons [11,12]. In earlier investigations, the focus was on establishing connections between driven-dissipative steady states and equilibrium many-body phases. These included the prediction of a phase transition from a superfluid to a Mott-insulator state for photons via the photon-blockade effect in coupled cavities [9,10,24–28]. More recently the focus was shifted towards the intriguing realm of the driven-dissipative regime, where nonequilibrium steady-state phases exhibit distinct properties in comparison to thermally equilibrium cases [29–31]. For example, the boundary between monostable and bistable phases in a driven-dissipative model resembles characteristic Mott insulator lobes, but the mean photon density is not constant within these regions [29]. In a wider context, various ideas and schemes have also been put forward to simulate geometric phases and gauge potentials for photons, opening the possibility for realizing nonequilibrium topological photonic states [32,33].

In this Letter, we investigate a driven-dissipative array of coupled nonlinear resonators with linearly increasing resonant frequencies (see Fig. 1). In our generic model, bosons are continuously injected into the system. Bosons are then redistributed via nearest-neighbor mode couplings until they eventually dissipate (for example, photon leakage through imperfect cavity mirrors). The dynamics of the system can

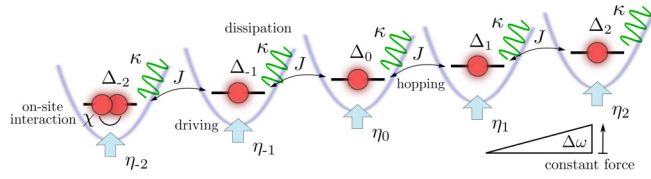


FIG. 1. Schematic sketch of the model consisting of an abstract array of driven-dissipative coupled nonlinear resonators with on-site interaction strength χ and linearly increasing detunings Δ_j , mimicking a constant force of $F = \Delta\omega$. Coherent pumps (η_j) inject bosons, which can hop between adjacent resonators at a constant rate J . Losses κ are modeled using the quantum Heisenberg equations (3).

be effectively captured by a driven-dissipative Bose-Hubbard model in a tilted potential *without* particle conservation. Despite the conceptual simplicity, the model, as we demonstrate, exhibits a variety of intriguing stationary and nonstationary, nonequilibrium phenomena controllable by the system parameters. A key result of our study is that, for sufficiently weak on-site interactions, bosons dynamically condense into a selected, spatially localized state due to explicit $U(1)$ symmetry breaking (Fig. 2), instead of exhibiting the expected

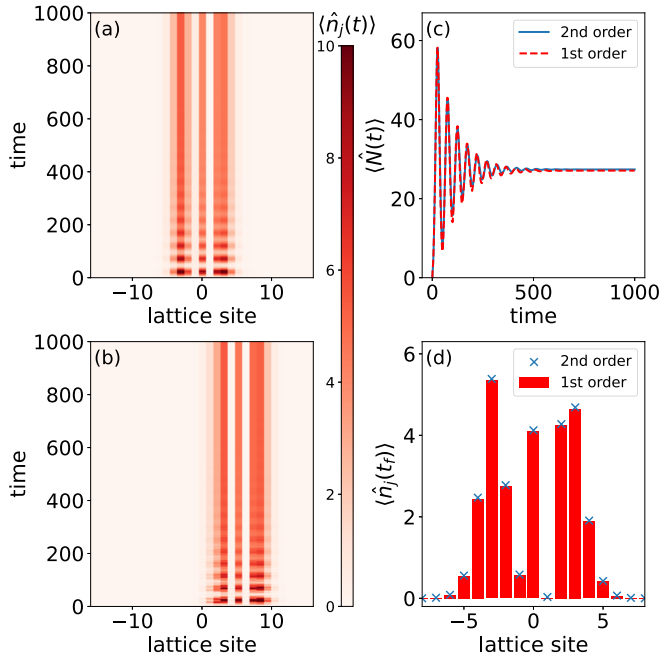


FIG. 2. Nonequilibrium dynamics of the system for a weak on-site interaction strength $\chi = 10^{-2}$ and the lattice tilt $\Delta\omega = 0.5$. The system reaches a spatially localized steady state in a long time. The expectation values of the particle number operators $\langle \hat{n}_j(t) \rangle$ in the course of time evolution in the first-order cumulant expansion (i.e., mean field) for (a) $j_0 = 0$ and (b) $j_0 = 5$. (c) The time evolution of the expectation value of the total boson number operator $\langle \hat{N}(t) \rangle$ for $j_0 = 0$ in both first- and second-order cumulant expansion. (d) The distribution of $\langle \hat{n}_j(t_f) \rangle$ over lattice sites in the stationary state for $j_0 = 0$ [cf. panel (a)]. To a very good approximation, the distribution is proportional to the probability density of a single WS state (see also Fig. 3), signaling a nonequilibrium Bose condensation into a WS state. The mean field is quite accurate in this weakly interacting regime.

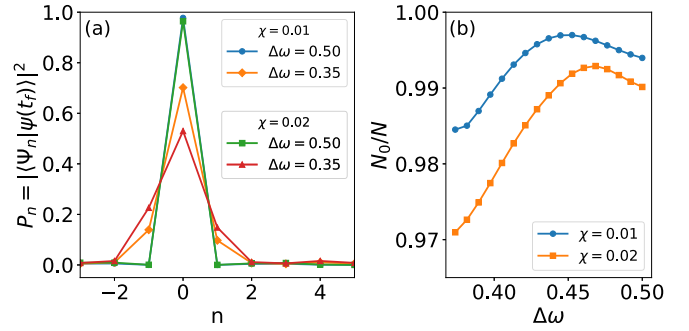


FIG. 3. (a) Steady-state fidelity $P_n(t_f)$ between the mean-field wave function $|\psi(t_f)\rangle$ and the WS basis states $|\Psi_n\rangle$. To a very good approximation, the condensate wave function is either proportional to only one WS state or is a superposition of a few WS states as in an antiresonant case (see the discussion in the main text). (b) The dominant eigenvalue N_0 of the single-particle density matrix as a function of $\Delta\omega$ remains close to the total number of bosons N , indicating a high-condensate fraction.

Bloch oscillations [34,35]. Specifically, the condensate wave function is often close to a single Wannier-Stark (WS) state, with only small contributions from neighboring WS states (Fig. 3). Interestingly, increasing the strength of local on-site interactions drives the system into a nonstationary regime (Fig. 4), where the bosonic density undergoes periodic Bloch-type oscillations over time which are induced by interactions (Fig. 5) [36–38]. This contrasts sharply with the irreversible decay of Bloch oscillations in interacting atoms within a one-dimensional tilted lattice [39–43]. Notably, both regimes are independent of initial conditions and the choice of the pumped resonator, stemming directly from the driven-dissipative nature of the system. The generic nature of our model suggests that experimental realization is feasible on various platforms, including superconducting circuits [44–46], photonic crystal structures [47], waveguide-coupled optical cavities [48], coupled photonic microcavities [49,50], exciton polariton lattices [51], cold atoms coupled to photonic crystals [52], and atom-filled transverse multimode cavities [53]. Although photonic implementation seems most promising, we note that such dynamics might also be observable for an ultracold gas in a vertical lattice with gravity or a tilted optical potential [54,55].

Model and its Hamiltonian. Consider an array of coupled resonators (labeled by $j \in \mathbb{Z}$) with linearly increasing resonant frequencies $\omega_j \propto j$, each containing a Kerr-like nonlinear medium. Coherent pumps with the frequency ω_p continuously inject bosons into the resonator modes. Each resonator is coupled to two adjacent resonators, which leads to a coherent hopping of bosons in the resonator lattice. The Hamiltonian of the system is given by [56] (see also Ref. [57] therein)

$$\hat{H} = \sum_j [\hbar\Delta_j \hat{a}_j^\dagger \hat{a}_j - J(\hat{a}_j^\dagger \hat{a}_{j+1} + \text{H.c.}) + \chi \hat{a}_j^{\dagger 2} \hat{a}_j^2] + \hbar \sum_j \eta_j (\hat{a}_j + \hat{a}_j^\dagger), \quad (1)$$

with \hat{a}_j and \hat{a}_j^\dagger being bosonic operators annihilating and creating a boson in the j th resonator, respectively. Here

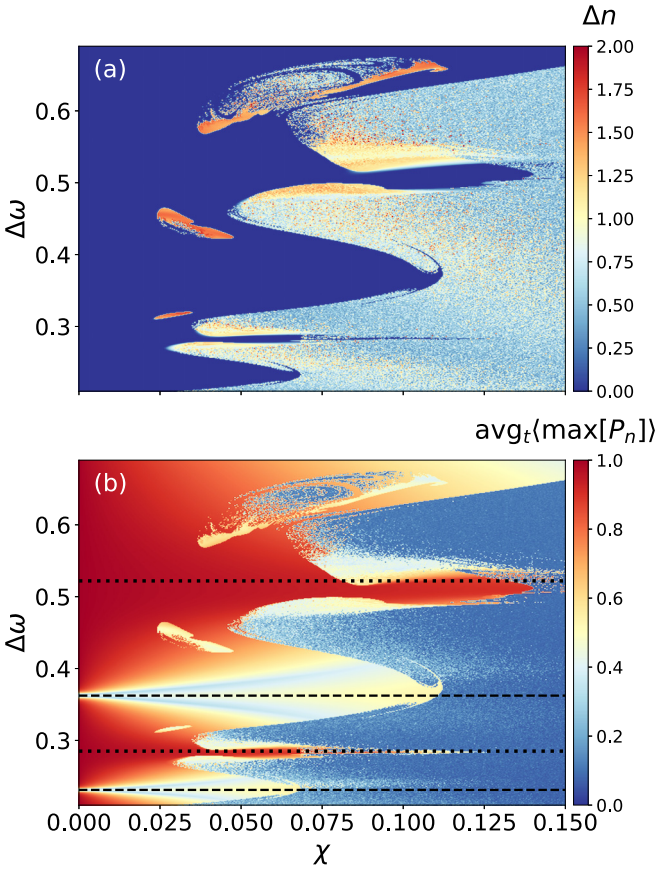


FIG. 4. Mean-field nonequilibrium many-body phase diagram of the system in the parameter plane of the force $\Delta\omega$ vs the on-site interaction strength χ . (a) Relative change of the total boson number over a long-time evolution Δn [Eq. (7)] reveals three regimes: stationary steady-state phase (deep blue), dynamically unstable chaotic regime (light blue), and nonstationary regular oscillatory states (warm colors). (b) Time-averaged maximal fidelity between the mean-field wave function $|\psi\rangle$ and the WS basis states $|\Psi_n\rangle$ is complementary to panel (a) and reveals particularly a series of narrow bands that can be explained on a single-particle level as pumping antiresonances; see the discussion in the main text. The dashed (dotted) lines correspond to zeros of the Bessel function \mathcal{J}_0 (\mathcal{J}_1). Note that interactions slightly shift the positions of the antiresonances.

we have defined

$$\Delta_j = \omega_j - \omega_p \equiv \Delta\omega(j - j_0) \quad (2)$$

as the resonator-pump detuning. Moreover, J is the nearest-neighbor tunneling-amplitude rate, χ is the on-site interaction strength due to the effective Kerr nonlinearity, and η_j is the pumping rate of the j th resonator. Bosonic losses κ , assumed to be the same throughout the lattice, are taken into account via the quantum Heisenberg equations of motion,

$$\frac{d\hat{a}_j}{dt} = \frac{i}{\hbar}[\hat{H}, \hat{a}_j] - \kappa\hat{a}_j. \quad (3)$$

The Hamiltonian (1) is an effective time-independent Hamiltonian expressed in the rotating frame of the coherent pumps, which is quite general and can be applied to many experimental scenarios (for example, such a Hamiltonian can be designed within a circuit-QED setup [45], but is also an

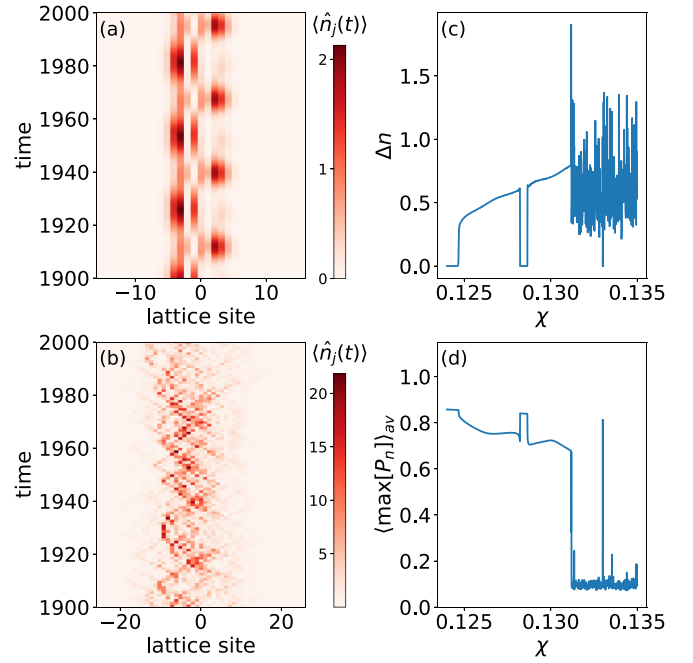


FIG. 5. Mean-field dynamics of the expectation values of the number operators $\langle \hat{n}_j(t) \rangle$ for different interaction strengths: (a) $\chi = 0.13$ in the oscillatory regime, and (b) $\chi = 0.135$ in the chaotic regime. Stationary and different nonstationary solutions are distinguished by monitoring (c) the relative change of the total boson number over a long-time evolution and (d) the time-averaged maximal fidelity. The lattice tilt is set to $\Delta\omega = 0.5$ for all panels.

effective lowest-Bloch-band Hamiltonian of ultracold atoms in driven dissipative optical lattices [55], see also Refs. [11,12]). The first line of the Hamiltonian (1) describes the familiar equilibrium Bose-Hubbard model in a tilted lattice. While in the noninteracting limit the equilibrium model features well-known Bloch oscillations [34,35], it has been recently shown that strong interactions can lead to disorder-free many-body localization [58,59] (for related experiments, see Ref. [60]). The second line of the Hamiltonian (1) introduces a coherent pumping, which along with the environment decay κ [see Eq. (3)] explicitly breaks the $U(1)$ symmetry of the system associated with the particle number conservation [56]. In the following we show that this lack of the particle conservation and the explicitly broken $U(1)$ symmetry due to the loss and gain processes have fundamental consequences in both statics and dynamics of the system.

Consequences of explicit $U(1)$ symmetry breaking: State selection. In order to gain some physical intuition, let us start with the noninteracting limit, $\chi = 0$. In the WS basis, the Heisenberg equations of motion read [56] as

$$i\frac{d\hat{b}_n}{dt} = (\Delta_n - i\kappa)\hat{b}_n + \tilde{\eta}_n, \quad (4)$$

where $\hat{b}_n = \sum_j \beta_{n,j}\hat{a}_n$, $\tilde{\eta}_n = \sum_j \beta_{n,j}\eta_j$, and $\beta_{n,j} = \mathcal{J}_{j-n}(2J/\Delta\omega)$, with \mathcal{J}_k being the Bessel function of the first kind of order k . The equations of motion (4) readily yield

$$\hat{b}_n(t) = e^{-it(\Delta_n - i\kappa)} \hat{b}_n(0) + \frac{e^{-it(\Delta_n - i\kappa)} - 1}{\Delta_n - i\kappa} \tilde{\eta}_n. \quad (5)$$

If $\forall_n \tilde{\eta}_n = 0$, the solutions correspond to damped Bloch oscillations [56]. If additionally $\kappa = 0$, one then recovers the common Bloch oscillations and the choice of j_0 in Eq. (2) becomes arbitrary as it only adds an irrelevant phase factor.

In the long-time limit $t \gg \kappa^{-1} \gg J^{-1}$, regardless of the choice of initial conditions $\hat{b}_n(0)$, the Bloch oscillations are completely damped out and the system reaches a steady state with the WS mode occupations,

$$\langle \hat{n}_n \rangle = \frac{\tilde{\eta}_n^2}{(\Delta\omega)^2(n - j_0)^2 + \kappa^2}. \quad (6)$$

As can be seen from Eq. (6), now j_0 plays an essential role. In particular, by properly choosing $j_0 \in \mathbb{Z}$, one can select dynamically a single WS mode ($n = j_0$) to be microscopically occupied. However, we note this approach does not work when $\tilde{\eta}_{j_0} = 0$, which happens for some specific ratios of $J/\Delta\omega$. In these cases, one encounters a sequence of pumping antiresonances, which leads to the occupation a few adjacent WS states instead. Furthermore, these antiresonances are responsible for nontrivial phase boundaries between stationary and nonstationary states as shown in Fig. 4, which we delve into in the last section.

The above simple analysis is valid qualitatively also for sufficiently small on-site interactions, which we confirm numerically in the following. In numerical simulations we set $J = \hbar = 1$ (as the unit of energy), $\kappa = 10^{-2}$, and $\forall_j \hat{a}_j(0) = 0$, and we calculate the expectation values of the relevant operators using the cumulant expansion in both first (i.e., mean field) and second order [56,61]. Moreover, for the sake of simplicity and without loss of generality, we consider only a single resonator pumping, $\eta_j = \eta\delta_{j,0}$, but different choices do not change our main conclusions [56]. Finally, with the exception of Fig. 2, we also fix $j_0 = 0$.

Nonequilibrium condensation in the weakly interacting regime. Now, we turn our attention to the weakly interacting regime, $\chi \ll 1$. As in the noninteracting case, in the weakly interacting regime, the many-body bosonic system still occupies macroscopically a single or a few one-particle WS states with a high degree of coherence. In Fig. 2, we show the expectation value of the number operators $\hat{n}_j = \hat{a}_j^\dagger \hat{a}_j$ as well as the total boson-number operator $\hat{N} = \sum_j \hat{n}_j$. As can be seen, in each case the system reaches a spatially localized stationary steady state which, for the chosen parameters, is proportional to a single WS state with $n = j_0$.

To further quantify this observation, we calculate the fidelity $P_n(t) = |\langle \Psi_n | \psi(t) \rangle|^2$ between the mean-field wave function $|\psi(t)\rangle$ and the WS basis states $|\Psi_n\rangle$. The distribution of P_n is illustrated in Fig. 3(a) in steady states, showing it is centered around $n = j_0 = 0$ [cf. Eq. (6)]. In general two distinct scenarios are possible: (i) The mean-field wave function consists predominantly of a single WS state, or (ii) it has contributions from a few different WS states. As Fig. 3(a) shows, for $\Delta\omega = 0.5$ [as in Figs. 2(a) and 2(d)] the wave function is close to the central WS state, while for $\Delta\omega = 0.35$ two additional modes $n = \pm 1$ are also significantly occupied at the macroscopic level. This is because of the aforementioned

pumping antiresonances, where the population of the $n = \pm 1$ ($n = 0$) mode is completely suppressed at $\Delta\omega \approx 0.522$ ($\Delta\omega \approx 0.362$) due to hitting a zero of the \mathcal{J}_1 (\mathcal{J}_0) Bessel function.

In order to confirm that we deal with Bose condensation, we consider the single-particle reduced density matrix $\hat{\rho}_1(x, x') = \langle \hat{\psi}^\dagger(x) \hat{\psi}(x') \rangle$, whose eigenvalues determine the occupation probabilities of the natural orbitals [62]. The highest occupation number quantifies the level of coherence in the system. Although we can expand the field operators in any orthogonal basis, we choose the Wannier basis $\hat{\psi}(x) = \sum_j w_j(x) \hat{a}_j$ and calculate the eigenvalues of $\langle \hat{a}_j^\dagger \hat{a}_l \rangle$ in a steady state of the system in the second-order cumulant expansion [56]. Indeed, as can be seen from Fig. 3(b), the highest eigenvalue N_0 is very close to the total number of bosons $N = \langle \hat{N} \rangle$, supporting the interpretation of a dynamical BEC. In contrast to the distribution of P_n as shown in Fig. 3(a), the highest eigenvalue of the reduced density matrix is only weakly affected by the lattice tilt $\Delta\omega$. Hence, we infer that the condensate wave function is either close to a single WS state or is a superposition of a few WS states.

Nonstationary phases in the strongly interacting regime. Above we showed that in the noninteracting and weakly interacting regimes bosons can condensate into a one or a few selected WS states and reach a steady state. However, with increasing the interaction strength χ , the stationary states lose their stability and intriguing nonstationary solutions appear. Figure 4(a) depicts the nonequilibrium many-body phase diagram of the system in the parameter plane of $\{\chi, \Delta\omega\}$ and contains three main regimes: stationary steady states (deep blue), a dynamically unstable chaotic regime (light blue), and nonstationary regular oscillatory states (warm colors). The three phases are distinguished by the relative change of the total boson number over a long-time evolution, defined as

$$\Delta n = \frac{\max_t \langle \hat{N}(t) \rangle - \min_t \langle \hat{N}(t) \rangle}{\text{avg}_t \langle \hat{N}(t) \rangle}, \quad (7)$$

with \max_t , \min_t , and avg_t denoting, respectively, the maximal, minimal, and average value of a quantum-averaged observable during a long-time evolution (where the initial transient dynamics of the system has been neglected). Although the phase diagram is dominated by the stationary and dynamically unstable chaotic regimes, regions of regular oscillatory dynamics appear mostly on boundaries between the two regimes (see also Fig. 4(b), showing the time-averaged maximal fidelity, and the Supplemental Material [56]).

Interestingly, bosons in the regular oscillatory regime tunnel between a few neighboring lattice sites performing spatially confined oscillations reminiscent of standard Bloch oscillations (see Fig. 5). Unlike standard Bloch oscillations that tend to decay in interacting systems [39–43], in our driven-dissipative model, oscillatory solutions are, in fact, induced by the on-site interactions and persist over long-time dynamics, even beyond the mean-field regime, although with quantitative differences [56], as expected from the literature [63,64]. These solutions can be conceptualized as multimode limit cycles (as shown in the Supplemental

Material [56]) within driven-dissipative systems, where the steady-state solutions of equations of motion exhibit dynamic instability [65–73].

Summary, conclusions, and perspectives. In summary, we studied an array of coupled nonlinear resonators with linearly increasing resonant frequencies, which is equivalent to a $U(1)$ -symmetry-broken driven-dissipative Bose-Hubbard model with a tilted potential. It could be equally implemented based on frequency-equidistant weakly coupled modes of a single resonator. Our semianalytical analysis reveals a range of both stationary and nonstationary nonequilibrium phenomena. Notably, bosons condense into selected, stationary WS states under sufficiently weak on-site interactions. As the strength of interactions increases, we observe a transition to a nonstationary dynamical regime marked by periodic Bloch-like oscillations over time. Unlike the equilibrium counterpart, these regular oscillations are induced by the interactions and do not decay over time.

Our research sheds light on the intricate behavior of driven-dissipative coupled resonator systems, emphasizing the role of explicit $U(1)$ symmetry breaking and interactions in shaping their dynamics. These findings hold promise for applications such as coherent light storage [74–76],

light confinement [77–79], generation of nonclassical many-photon states [80–82], and distributed quantum sensing [83–85]. While our focus in this Letter has been on weakly interacting systems, we underscore the importance of delving deeper into dynamics beyond perturbation regimes. Specifically, it is interesting to explore the nonstationary states in many-body regimes, particularly in the context of ergodicity breaking [86,87] and Stark many-body localization [88]. Another intriguing scenario is to extend our driven-dissipative model to a topological setting, where exotic nonequilibrium topological effects are expected to appear [89–92].

The data presented in this article are available from Ref. [93].

Acknowledgments. We acknowledge stimulating discussions with Darrick Chang and Thomas Pohl. This research was funded in whole or in part by the Austrian Science Fund (FWF) [Grant DOIs 10.55776/ESP171, 10.55776/M3304, and 10.55776/P35891]. F.M. additionally acknowledges the support of the ESQ-Discovery Grant of the Austrian Academy of Sciences (ÖAW).

-
- [1] H. A. Gersch and G. C. Knollman, Quantum cell model for bosons, *Phys. Rev.* **129**, 959 (1963).
 - [2] O. Dutta, M. Gajda, P. Hauke, M. Lewenstein, D.-S. Lühmann, B. A. Malomed, T. Sowiński, and J. Zakrzewski, Non-standard Hubbard models in optical lattices: A review, *Rep. Prog. Phys.* **78**, 066001 (2015).
 - [3] H. Miyazaki, Y. Takahide, A. Kanda, and Y. Ootuka, Quantum fluctuations and dissipative phase transition in one-dimensional Josephson junction arrays, *Phys. E (Amsterdam, Neth.)* **18**, 41 (2003).
 - [4] F. Vicentini, F. Minganti, R. Rota, G. Orso, and C. Ciuti, Critical slowing down in driven-dissipative Bose-Hubbard lattices, *Phys. Rev. A* **97**, 013853 (2018).
 - [5] D. Roberts and A. A. Clerk, Competition between two-photon driving, dissipation, and interactions in bosonic lattice models: An exact solution, *Phys. Rev. Lett.* **130**, 063601 (2023).
 - [6] M. Kiffner and M. J. Hartmann, Dissipation-induced correlations in one-dimensional bosonic systems, *New J. Phys.* **13**, 053027 (2011).
 - [7] A. Krzywicka and T. Polak, Coexistence of two kinds of superfluidity at finite temperatures in optical lattices, *Ann. Phys.* **443**, 168973 (2022).
 - [8] A. Krzywicka and T. P. Polak, Reentrant phase behavior in systems with density-induced tunneling, *Sci. Rep.* **14**, 10364 (2024).
 - [9] M. J. Hartmann, F. G. S. L. Brandão, and M. B. Plenio, Strongly interacting polaritons in coupled arrays of cavities, *Nat. Phys.* **2**, 849 (2006).
 - [10] A. D. Greentree, C. Tahan, J. H. Cole, and L. C. L. Hollenberg, Quantum phase transitions of light, *Nat. Phys.* **2**, 856 (2006).
 - [11] C. Noh and D. G. Angelakis, Quantum simulations and many-body physics with light, *Rep. Prog. Phys.* **80**, 016401 (2017).
 - [12] M. J. Hartmann, Quantum simulation with interacting photons, *J. Opt.* **18**, 104005 (2016).
 - [13] D. F. Walls and G. F. Milburn, *Quantum Optics* (Springer, Berlin, 2008).
 - [14] H. Deng, H. Haug, and Y. Yamamoto, Exciton-polariton Bose-Einstein condensation, *Rev. Mod. Phys.* **82**, 1489 (2010).
 - [15] J. Keeling and N. G. Berloff, Exciton-polariton condensation, *Contemp. Phys.* **52**, 131 (2011).
 - [16] T. Byrnes, N. Y. Kim, and Y. Yamamoto, Exciton-polariton condensates, *Nat. Phys.* **10**, 803 (2014).
 - [17] F. Mivehvar, F. Piazza, T. Donner, and H. Ritsch, Cavity QED with quantum gases: New paradigms in many-body physics, *Adv. Phys.* **70**, 1 (2021).
 - [18] I. Carusotto and C. Ciuti, Quantum fluids of light, *Rev. Mod. Phys.* **85**, 299 (2013).
 - [19] H. Deng, G. Weihs, C. Santori, J. Bloch, and Y. Yamamoto, Condensation of semiconductor microcavity exciton polaritons, *Science* **298**, 199 (2002).
 - [20] J. Kasprzak, M. Richard, S. Kundermann, A. Baas, P. Jeambrun, J. M. J. Keeling, F. M. Marchetti, M. H. Szymańska, R. André, J. L. Staehli, V. Savona, P. B. Littlewood, B. Deveaud, and L. S. Dang, Bose-Einstein condensation of exciton polaritons, *Nature (London)* **443**, 409 (2006).
 - [21] R. Balili, V. Hartwell, D. Snoke, L. Pfeiffer, and K. West, Bose-Einstein condensation of microcavity polaritons in a trap, *Science* **316**, 1007 (2007).
 - [22] A. Amo, J. Lefrère, S. Pigeon, C. Adrados, C. Ciuti, I. Carusotto, R. Houdré, E. Giacobino, and A. Bramati, Superfluidity of polaritons in semiconductor microcavities, *Nat. Phys.* **5**, 805 (2009).

- [23] J. Klaers, J. Schmitt, F. Vewinger, and M. Weitz, Bose–Einstein condensation of photons in an optical microcavity, *Nature (London)* **468**, 545 (2010).
- [24] M. J. Hartmann, F. G. S. L. Brandão, and M. B. Plenio, Quantum many-body phenomena in coupled cavity arrays, *Laser Photon. Rev.* **2**, 527 (2008).
- [25] S. Schmidt and G. Blatter, Strong coupling theory for the Jaynes-Cummings-Hubbard model, *Phys. Rev. Lett.* **103**, 086403 (2009).
- [26] A. Tomadin, V. Giovannetti, R. Fazio, D. Gerace, I. Carusotto, H. E. Türeci, and A. Imamoglu, Signatures of the superfluid-insulator phase transition in laser-driven dissipative nonlinear cavity arrays, *Phys. Rev. A* **81**, 061801(R) (2010).
- [27] C.-W. Wu, M. Gao, Z.-J. Deng, H.-Y. Dai, P.-X. Chen, and C.-Z. Li, Quantum phase transition of light in a one-dimensional photon-hopping-controllable resonator array, *Phys. Rev. A* **84**, 043827 (2011).
- [28] Although these models share many similarities, such as bosons hopping coherently between nearest-neighbor sites with local nonlinearities, we note that quantitative differences may arise on different energy scales.
- [29] A. L. Boité, G. Orso, and C. Ciuti, Steady-state phases and tunneling-induced instabilities in the driven dissipative Bose-Hubbard model, *Phys. Rev. Lett.* **110**, 233601 (2013).
- [30] A. L. Boité, G. Orso, and C. Ciuti, Bose-Hubbard model: Relation between driven-dissipative steady states and equilibrium quantum phases, *Phys. Rev. A* **90**, 063821 (2014).
- [31] T. Graß, Excitations and correlations in the driven-dissipative Bose-Hubbard model, *Phys. Rev. A* **99**, 043607 (2019).
- [32] L. Lu, J. D. Joannopoulos, and M. Soljačić, Topological photonics, *Nat. Photon.* **8**, 821 (2014).
- [33] T. Ozawa, H. M. Price, A. Amo, N. Goldman, M. Hafezi, L. Lu, M. C. Rechtsman, D. Schuster, J. Simon, O. Zilberberg, and I. Carusotto, Topological photonics, *Rev. Mod. Phys.* **91**, 015006 (2019).
- [34] G. H. Wannier, Wave functions and effective Hamiltonian for Bloch electrons in an electric field, *Phys. Rev.* **117**, 432 (1960).
- [35] T. Hartmann, F. Keck, H. J. Korsch, and S. Mossmann, Dynamics of Bloch oscillations, *New J. Phys.* **6**, 2 (2004).
- [36] U. Peschel, T. Pertsch, and F. Lederer, Optical Bloch oscillations in waveguide arrays, *Opt. Lett.* **23**, 1701 (1998).
- [37] R. Sapienza, P. Costantino, D. Wiersma, M. Ghulinyan, C. J. Oton, and L. Pavesi, Optical analogue of electronic Bloch oscillations, *Phys. Rev. Lett.* **91**, 263902 (2003).
- [38] L. Yuan and S. Fan, Bloch oscillation and unidirectional translation of frequency in a dynamically modulated ring resonator, *Optica* **3**, 1014 (2016).
- [39] A. Buchleitner and A. R. Kolovsky, Interaction-induced decoherence of atomic Bloch oscillations, *Phys. Rev. Lett.* **91**, 253002 (2003).
- [40] M. Gustavsson, E. Haller, M. J. Mark, J. G. Danzl, G. Rojas-Kopeinig, and H.-C. Nägerl, Control of interaction-induced dephasing of Bloch oscillations, *Phys. Rev. Lett.* **100**, 080404 (2008).
- [41] D. O. Krimer, R. Khomeriki, and S. Flach, Delocalization and spreading in a nonlinear Stark ladder, *Phys. Rev. E* **80**, 036201 (2009).
- [42] M. Eckstein and P. Werner, Damping of Bloch oscillations in the Hubbard model, *Phys. Rev. Lett.* **107**, 186406 (2011).
- [43] However, note that bound states of a few strongly interacting particles can experience fractional Bloch oscillations at frequencies that are multiples of single-particle Bloch oscillations [94–97] (for experiments, see Refs. [98,99]). Also, the decay of Bloch oscillations and the emergence of the directional motion in the excitation phonon have been recently reported in Ref. [100].
- [44] A. A. Houck, H. E. Türeci, and J. Koch, On-chip quantum simulation with superconducting circuits, *Nat. Phys.* **8**, 292 (2012).
- [45] J. Jin, D. Rossini, R. Fazio, M. Leib, and M. J. Hartmann, Photon solid phases in driven arrays of nonlinearly coupled cavities, *Phys. Rev. Lett.* **110**, 163605 (2013).
- [46] J. Jin, D. Rossini, M. Leib, M. J. Hartmann, and R. Fazio, Steady-state phase diagram of a driven QED-cavity array with cross-Kerr nonlinearities, *Phys. Rev. A* **90**, 023827 (2014).
- [47] A. Majumdar, A. Rundquist, M. Bajcsy, V. D. Dasika, S. R. Bank, and J. Vučković, Design and analysis of photonic crystal coupled cavity arrays for quantum simulation, *Phys. Rev. B* **86**, 195312 (2012).
- [48] G. Lepert, M. Trupke, M. J. Hartmann, M. B. Plenio, and E. A. Hinds, Arrays of waveguide-coupled optical cavities that interact strongly with atoms, *New J. Phys.* **13**, 113002 (2011).
- [49] Y.-F. Xiao, V. Gaddam, and L. Yang, Coupled optical microcavities: An enhanced refractometric sensing configuration, *Opt. Express* **16**, 12538 (2008).
- [50] S. R. K. Rodriguez, A. Amo, I. Sagnes, L. Le Gratiet, E. Galopin, A. Lemaître, and J. Bloch, Interaction-induced hopping phase in driven-dissipative coupled photonic microcavities, *Nat. Commun.* **7**, 11887 (2016).
- [51] C. Schneider, K. Winkler, M. D. Fraser, M. Kamp, Y. Yamamoto, E. A. Ostrovskaya, and S. Höfling, Exciton-polariton trapping and potential landscape engineering, *Rep. Prog. Phys.* **80**, 016503 (2017).
- [52] J. S. Douglas, H. Habibian, C.-L. Hung, A. V. Gorshkov, H. J. Kimble, and D. E. Chang, Quantum many-body models with cold atoms coupled to photonic crystals, *Nat. Photon.* **9**, 326 (2015).
- [53] A. J. Kollár, A. T. Papageorge, K. Baumann, M. A. Armen, and B. L. Lev, An adjustable-length cavity and Bose–Einstein condensate apparatus for multimode cavity QED, *New J. Phys.* **17**, 043012 (2015).
- [54] M. Zelan, H. Hagman, K. Karlsson, C. M. Dion, and A. Kastberg, Fluctuation-induced drift in a gravitationally tilted optical lattice, *Phys. Rev. E* **82**, 031136 (2010).
- [55] V. Sharma and E. J. Mueller, Driven-dissipative control of cold atoms in tilted optical lattices, *Phys. Rev. A* **103**, 043322 (2021).
- [56] See Supplemental Material at <http://link.aps.org/supplemental/10.1103/PhysRevB.110.L100303> for the derivation of the rotating frame Hamiltonian, discussion of Wannier-Stark states and the $U(1)$ symmetry breaking terms, details of the cumulant expansion, and more examples of interaction-induced Bloch oscillations within and beyond the mean-field regime.

- [57] I. Bloch, J. Dalibard, and W. Zwerger, Many-body physics with ultracold gases, *Rev. Mod. Phys.* **80**, 885 (2008).
- [58] R. Yao and J. Zakrzewski, Many-body localization of bosons in an optical lattice: Dynamics in disorder-free potentials, *Phys. Rev. B* **102**, 104203 (2020).
- [59] S. R. Taylor, M. Schulz, F. Pollmann, and R. Moessner, Experimental probes of Stark many-body localization, *Phys. Rev. B* **102**, 054206 (2020).
- [60] W. Morong, F. Liu, P. Becker, K. S. Collins, L. Feng, A. Kyprianidis, G. Pagano, T. You, A. V. Gorshkov, and C. Monroe, Observation of Stark many-body localization without disorder, *Nature (London)* **599**, 393 (2021).
- [61] D. Plankensteiner, C. Hotter, and H. Ritsch, QuantumCumulants.jl: A Julia framework for generalized mean-field equations in open quantum systems, *Quantum* **6**, 617 (2022).
- [62] C. J. Pethick and H. Smith, *Bose–Einstein Condensation in Dilute Gases* (Cambridge University, Cambridge, England, 2008).
- [63] T. P. Polak and T. K. Kopeć, Local dissipation effects in two-dimensional quantum Josephson junction arrays with a magnetic field, *Phys. Rev. B* **72**, 014509 (2005).
- [64] D. Huybrechts, F. Minganti, F. Nori, M. Wouters, and N. Shammah, Validity of mean-field theory in a dissipative critical system: Liouvillian gap, $\mathbb{P}\mathbb{T}$ -symmetric antigap, and permutational symmetry in the XYZ model, *Phys. Rev. B* **101**, 214302 (2020).
- [65] F. Piazza and H. Ritsch, Self-ordered limit cycles, chaos, and phase slippage with a superfluid inside an optical resonator, *Phys. Rev. Lett.* **115**, 163601 (2015).
- [66] C.-K. Chan, T. E. Lee, and S. Gopalakrishnan, Limit-cycle phase in driven-dissipative spin systems, *Phys. Rev. A* **91**, 051601(R) (2015).
- [67] E. T. Owen, J. Jin, D. Rossini, R. Fazio, and M. J. Hartmann, Quantum correlations and limit cycles in the driven-dissipative Heisenberg lattice, *New J. Phys.* **20**, 045004 (2018).
- [68] H. Keßler, J. G. Cosme, M. Hemmerling, L. Mathey, and A. Hemmerich, Emergent limit cycles and time crystal dynamics in an atom-cavity system, *Phys. Rev. A* **99**, 053605 (2019).
- [69] E. Colella, A. Kosior, F. Mivehvar, and H. Ritsch, Open quantum system simulation of Faraday’s induction law via dynamical instabilities, *Phys. Rev. Lett.* **128**, 070603 (2022).
- [70] P. Gao, Z.-W. Zhou, G.-C. Guo, and X.-W. Luo, Self-organized limit cycles in red-detuned atom-cavity systems, *Phys. Rev. A* **107**, 023311 (2023).
- [71] A. Kosior, H. Ritsch, and F. Mivehvar, Nonequilibrium phases of ultracold bosons with cavity-induced dynamic gauge fields, *SciPost Phys.* **15**, 046 (2023).
- [72] F. Mivehvar, Conventional and unconventional Dicke models: Multistabilities and nonequilibrium dynamics, *Phys. Rev. Lett.* **132**, 073602 (2024).
- [73] J. Skulte, P. Kongkhambut, H. Keßler, A. Hemmerich, L. Mathey, and J. G. Cosme, Realizing limit cycles in dissipative bosonic systems, *Phys. Rev. A* **109**, 063317 (2024).
- [74] D. F. Phillips, A. Fleischhauer, A. Mair, R. L. Walsworth, and M. D. Lukin, Storage of light in atomic vapor, *Phys. Rev. Lett.* **86**, 783 (2001).
- [75] Y. O. Dudin, L. Li, and A. Kuzmich, Light storage on the time scale of a minute, *Phys. Rev. A* **87**, 031801(R) (2013).
- [76] O. Katz and O. Firstenberg, Light storage for one second in room-temperature alkali vapor, *Nat. Commun.* **9**, 2074 (2018).
- [77] H. Cao, J. Y. Xu, D. Z. Zhang, S.-H. Chang, S. T. Ho, E. W. Seelig, X. Liu, and R. P. H. Chang, Spatial confinement of laser light in active random media, *Phys. Rev. Lett.* **84**, 5584 (2000).
- [78] M. Notomi, Strong light confinement with periodicity, *Proc. IEEE* **99**, 1768 (2011).
- [79] F. Riboli, N. Caselli, S. Vignolini, F. Intonti, K. Vynck, P. Barthelemy, A. Gerardino, L. Balet, L. H. Li, A. Fiore, M. Gurioli, and D. S. Wiersma, Engineering of light confinement in strongly scattering disordered media, *Nat. Mater.* **13**, 720 (2014).
- [80] M. Cooper, L. J. Wright, C. Söller, and B. J. Smith, Experimental generation of multi-photon Fock states, *Opt. Express* **21**, 5309 (2013).
- [81] D. E. Chang, V. Vuletić, and M. D. Lukin, Quantum nonlinear optics—photon by photon, *Nat. Photon.* **8**, 685 (2014).
- [82] A. Pizzi, A. Gorlach, N. Rivera, A. Nunnenkamp, and I. Kaminer, Light emission from strongly driven many-body systems, *Nat. Phys.* **19**, 551 (2023).
- [83] X. Guo, C. R. Breum, J. Borregaard, S. Izumi, M. V. Larsen, T. Gehring, M. Christandl, J. S. Neergaard-Nielsen, and U. L. Andersen, Distributed quantum sensing in a continuous-variable entangled network, *Nat. Phys.* **16**, 281 (2020).
- [84] Z. Zhang and Q. Zhuang, Distributed quantum sensing, *Quantum Sci. Technol.* **6**, 043001 (2021).
- [85] J. C. Pelayo, K. Gietka, and T. Busch, Distributed quantum sensing with optical lattices, *Phys. Rev. A* **107**, 033318 (2023).
- [86] A. D. Luca and A. Scardicchio, Ergodicity breaking in a model showing many-body localization, *Europhys. Lett.* **101**, 37003 (2013).
- [87] K. Gietka, J. Chwedeńczuk, T. Wasak, and F. Piazza, Multiparticle entanglement dynamics in a regular-to-ergodic transition: Quantum Fisher information approach, *Phys. Rev. B* **99**, 064303 (2019).
- [88] M. Schulz, C. A. Hooley, R. Moessner, and F. Pollmann, Stark many-body localization, *Phys. Rev. Lett.* **122**, 040606 (2019).
- [89] M. Hafezi, S. Mittal, J. Fan, A. Migdall, and J. M. Taylor, Imaging topological edge states in silicon photonics, *Nat. Photon.* **7**, 1001 (2013).
- [90] S. Mittal, J. Fan, S. Faez, A. Migdall, J. M. Taylor, and M. Hafezi, Topologically robust transport of photons in a synthetic gauge field, *Phys. Rev. Lett.* **113**, 087403 (2014).
- [91] Z. Gong, Y. Ashida, K. Kawabata, K. Takasan, S. Higashikawa, and M. Ueda, Topological phases of non-Hermitian systems, *Phys. Rev. X* **8**, 031079 (2018).
- [92] E. Colella, F. Mivehvar, F. Piazza, and H. Ritsch, Hofstadter butterfly in a cavity-induced dynamic synthetic magnetic field, *Phys. Rev. B* **100**, 224306 (2019).

- [93] A. Kosior, K. Gietka, F. Mivehvar, and H. Ritsch, Nonequilibrium nonlinear effects and dynamical boson condensation in a driven-dissipative Wannier-Stark lattice [Data set], Zenodo (2024), <https://zenodo.org/doi/10.5281/zenodo.10986261>.
- [94] F. Claro, J. F. Weisz, and S. Curilef, Interaction-induced oscillations in correlated electron transport, *Phys. Rev. B* **67**, 193101 (2003).
- [95] W. S. Dias, E. M. Nascimento, M. L. Lyra, and F. A. B. F. de Moura, Frequency doubling of Bloch oscillations for interacting electrons in a static electric field, *Phys. Rev. B* **76**, 155124 (2007).
- [96] R. Khomeriki, D. O. Krimer, M. Haque, and S. Flach, Interaction-induced fractional Bloch and tunneling oscillations, *Phys. Rev. A* **81**, 065601 (2010).
- [97] D. Wiater, T. Sowiński, and J. Zakrzewski, Two bosonic quantum walkers in one-dimensional optical lattices, *Phys. Rev. A* **96**, 043629 (2017).
- [98] G. Corrielli, A. Crespi, G. D. Valle, S. Longhi, and R. Osellame, Fractional Bloch oscillations in photonic lattices, *Nat. Commun.* **4**, 1555 (2013).
- [99] P. M. Preiss, R. Ma, M. E. Tai, A. Lukin, M. Rispoli, P. Zupancic, Y. Lahini, R. Islam, and M. Greiner, Strongly correlated quantum walks in optical lattices, *Science* **347**, 1229 (2015).
- [100] A. Kosior, S. Kokkelmans, M. Lewenstein, J. Zakrzewski, and M. Płodzień, Phonon-assisted coherent transport of excitations in Rydberg-dressed atom arrays, *Phys. Rev. A* **108**, 043308 (2023).